



Article

# Multi-Scale Effects of Meteorological Conditions and Anthropogenic Emissions on PM<sub>2.5</sub> Concentrations over Major Cities of the Yellow River Basin

Jiejun Zhang <sup>1,†</sup>, Pengfei Liu <sup>1,2,3,\*,†</sup> , Hongquan Song <sup>2,3,4,\*</sup> , Changhong Miao <sup>1</sup>, Jie Yang <sup>1</sup>, Longlong Zhang <sup>2</sup>, Junwu Dong <sup>5</sup>, Yi Liu <sup>1</sup>, Yunlong Zhang <sup>2</sup> and Bingchen Li <sup>2</sup>

- <sup>1</sup> Key Research Institute of Yellow River Civilization and Sustainable Development & Collaborative Innovation Center on Yellow River Civilization of Henan Province, Henan University, Kaifeng 475004, China
- <sup>2</sup> College of Geography and Environmental Science, Henan University, Kaifeng 475004, China
- <sup>3</sup> Institute of Urban Big Data, Henan University, Kaifeng 475004, China
- <sup>4</sup> Key Laboratory of Geospatial Technology for the Middle and Lower Yellow River Regions (Henan University), Ministry of Education, Kaifeng 475004, China
- <sup>5</sup> College of Resource Environment and Tourism, Capital Normal University, Beijing 100048, China
- \* Correspondence: lpf@henu.edu.cn (P.L.); hqsong@henu.edu.cn (H.S.)
- † These authors contributed equally to this work and should be considered co-first authors.

**Abstract:** The mechanism behind PM<sub>2.5</sub> pollution is complex, and its performance at multi-scales is still unclear. Based on PM<sub>2.5</sub> monitoring data collected from 2015 to 2021, we used the GeoDetector model to assess the multi-scale effects of meteorological conditions and anthropogenic emissions, as well as their interactions with PM<sub>2.5</sub> concentrations in major cities in the Yellow River Basin (YRB). Our study confirms that PM<sub>2.5</sub> concentrations in the YRB from 2015 to 2021 show an inter-annual and inter-season decreasing trend and that PM<sub>2.5</sub> concentrations varied more significantly in winter. The inter-month variation of PM<sub>2.5</sub> concentrations shows a sinusoidal pattern from 2015 to 2021, with the highest concentrations in January and December and the lowest from June to August. The PM<sub>2.5</sub> concentrations for major cities in the middle and downstream regions of the YRB are higher than in the upper areas, with high spatial distribution in the east and low spatial distribution in the west. Anthropogenic emissions and meteorological conditions have similar inter-annual effects, while air pressure and temperature are the two main drivers across the whole basin. At the sub-basin scale, meteorological conditions have stronger inter-annual effects on PM<sub>2.5</sub> concentrations, of which temperature is the dominant impact factor. Wind speed has a significant effect on PM<sub>2.5</sub> concentrations across the four seasons in the downstream region and has the strongest effect in winter. Primary PM<sub>2.5</sub> and ammonia are the two main emission factors. Interactions between the factors significantly enhanced the PM<sub>2.5</sub> concentrations. The interaction between ammonia and other emissions plays a dominant role at the whole and sub-basin scales in summer, while the interaction between meteorological factors plays a dominant role at the whole-basin scale in winter. Our study not only provides cases and references for the development of PM<sub>2.5</sub> pollution prevention and control policies in YRB but can also shed light on similar regions in China as well as in other regions of the world.

**Keywords:** air pollution; PM<sub>2.5</sub>; GeoDetector model; interactive effects; the Yellow River Basin



**Citation:** Zhang, J.; Liu, P.; Song, H.; Miao, C.; Yang, J.; Zhang, L.; Dong, J.; Liu, Y.; Zhang, Y.; Li, B. Multi-Scale Effects of Meteorological Conditions and Anthropogenic Emissions on PM<sub>2.5</sub> Concentrations over Major Cities of the Yellow River Basin. *Int. J. Environ. Res. Public Health* **2022**, *19*, 15060. <https://doi.org/10.3390/ijerph192215060>

Academic Editor: Benoit Nemery

Received: 16 September 2022

Accepted: 14 November 2022

Published: 16 November 2022

**Publisher's Note:** MDPI stays neutral with regard to jurisdictional claims in published maps and institutional affiliations.



**Copyright:** © 2022 by the authors. Licensee MDPI, Basel, Switzerland. This article is an open access article distributed under the terms and conditions of the Creative Commons Attribution (CC BY) license (<https://creativecommons.org/licenses/by/4.0/>).

## 1. Introduction

With the acceleration of industrialization and urbanization, China's economy has grown steadily; at the same time, the emissions of greenhouse gases and air pollutants have also continued to increase [1–3]. As the most urgent threat to public health and the ecosystem, PM<sub>2.5</sub> (particulate matter of less than 2.5 μm in diameter) has become a major air pollutant in China [4–9]. In order to effectively deal with the serious PM<sub>2.5</sub>

pollution problem, since 2013, the Chinese government has implemented a series of air pollution prevention and control measures that have achieved considerable results [10,11]. However, the pollution factors of PM<sub>2.5</sub> concentrations are complex and there is variability at different spatial and temporal scales, which leads to uncertainty in the effectiveness of the implementation of air pollution prevention and control measures [12]. Therefore, conducting an analysis of PM<sub>2.5</sub> pollution impact mechanisms, especially the performance of PM<sub>2.5</sub> concentrations and impact factors in typical regions at different spatial and temporal scales, will have implications for the formulation of precise air pollution prevention and control policies.

PM<sub>2.5</sub> concentrations are affected by a variety of factors, including natural and socioeconomic factors [3,11]. Meteorological conditions (MC<sub>S</sub>) are important factors affecting the accumulation, dispersion, and chemical processes of pollutants. Temperature [13–16], relative humidity [17–19], precipitation [15,20,21], wind speed [22], sunshine duration [23], and surface air pressure [14] have significant effects on PM<sub>2.5</sub> concentrations. In addition, anthropogenic emissions (AE<sub>S</sub>) from industrial, transportation, agricultural, and residential sectors also have a significant influence on PM<sub>2.5</sub> concentrations. Anthropogenic precursors, such as sulfur dioxide, nitrogen oxide, volatile organic compounds, and ammonia, aggravate PM<sub>2.5</sub> pollution by generating secondary aerosols through a series of photochemical reactions [12,16,24,25]. Numerous studies have also analyzed the impact of PM<sub>2.5</sub> concentrations in terms of urbanization [26–28], urban form [29–32], and industrial structure [33,34].

The Chinese government has been publicly releasing air pollution site-monitoring data since 2013, which has made it possible for scholars to conduct air pollution-related studies at a national scale [3,35,36]. Meanwhile, some scholars have also conducted analyses focusing on developed regions with serious air pollution, such as Beijing-Tianjin-Hebei in northern China [12,16,37–39], the Yangtze River Delta in central China [40–43], the Pearl River Delta in southern China [44–47], and the Chengdu-Chongqing urban agglomeration in southwest China [21,48,49].

The Yellow River Basin (YRB) is an important energy, chemical, raw material, and general industrial base in northern China, as well as an ecological corridor connecting the Qinghai–Tibet Plateau, the Loess Plateau, and the North China Plain. With its accelerated urbanization, the YRB faces serious air pollution issues, mainly due to particulate matter [50]. The Fenwei Plain in the YRB became one of the three key areas for air pollution control in China in 2018, replacing the Pearl River Delta [51]. In recent years, some scholars have explored the spatial and temporal characteristics and driving mechanisms behind air pollution, focusing on key cities [26,52–54], major regions, and urban agglomerations [51,55–57] in the YRB. Wang et al. [58] studied the causes of heavy haze pollution in Xi'an, Shaanxi Province, and found that high-intensity anthropogenic emissions, relative humidity, consistent low temperature, and surface air pressure were the main drivers of heavy pollution formation. He et al. [59] studied the characteristics and source resolution of water-soluble inorganic ion species in PM<sub>2.5</sub> in Taiyuan, Shanxi Province, China, and found that Mg<sup>2+</sup> and Ca<sup>2+</sup> were derived not only from soil dust but also from coal combustion and industrial emissions. Meanwhile, wind speed also affected the transport of dust and, thus, had an impact on PM<sub>2.5</sub> and water-soluble inorganic ions. In general, scholars have conducted studies on scientific issues related to atmospheric pollution in the YRB. However, due to the complexity of the natural geographical conditions and anthropogenic emissions in the YRB, the impact mechanisms of air pollution have still not been sufficiently discussed. Most of the current studies have conducted a relative analysis based on one aspect of the natural and socioeconomic factors at a single spatial and temporal scale. However, analyses that explore the multi-scale mechanisms influencing PM<sub>2.5</sub> concentrations in the YRB, which integrate natural and socioeconomic factors, are still lacking.

Therefore, we took the YRB as the study area and used the GeoDetector model to investigate the multi-scale effects of meteorological conditions and anthropogenic emissions

and their interactions on PM<sub>2.5</sub> concentrations. The main objectives of this research are as follows: (1) to identify the spatial and temporal distribution patterns of PM<sub>2.5</sub> concentrations in the YRB; (2) to elucidate the effects of meteorological conditions and anthropogenic emissions on PM<sub>2.5</sub> concentrations at different spatial and temporal scales; (3) to analyze the effect of the interaction between meteorological conditions and anthropogenic emissions on PM<sub>2.5</sub> concentrations. Our study could provide insight into the mechanism of PM<sub>2.5</sub> pollution in the YRB and bear out the formulation of air pollution prevention and control policies, as well as a reference for air pollution management in similar basins in China and other developing countries.

## 2. Materials and Methods

### 2.1. Study Area

The YRB is located in the north of China, with a total length of 5464 km. It holds a very important position in terms of economic development and ecological security, as an important ecological barrier, and as an important economic belt in China. We have adopted the Yellow River Basin boundary identified by the Chinese National Strategy for Ecological Protection and Quality Development, involving 91 prefectural-level administrative regions. The region includes the entirety of seven provinces in Qinghai, Gansu, Ningxia, Shaanxi, Shanxi, Henan, and Shandong, as well as six cities and one union in western Inner Mongolia and two states in Sichuan, Aba, and Ganzi (Figure 1). We divided the YRB into three sub-basins, based on provincial administrative units: the Upper Yellow River Basin (UYR), including 7 cities (leagues) in Qinghai, Gansu, Ningxia, and Inner Mongolia and 2 states in Sichuan, the Middle Yellow River Basin (MYR), including Shanxi and Shaanxi, and the downstream area of the Yellow River Basin (DYR), including Henan and Shandong.

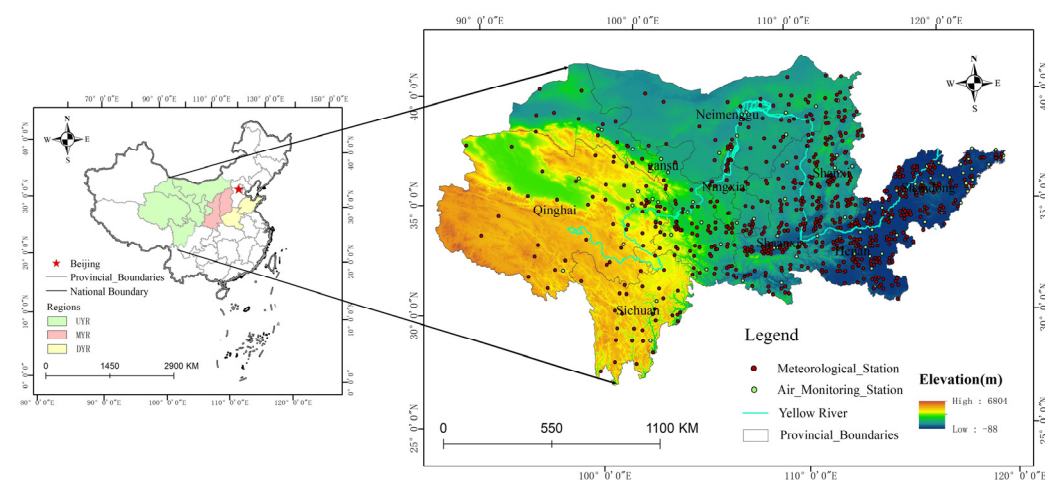


**Figure 1.** Overview of the Yellow River Basin in China. (YRB denotes the Yellow River Basin; UYR denotes the Upper Yellow River Basin; MYR denotes the Middle Yellow River Basin; DYR denotes the downstream area of the Yellow River Basin).

The YRB spans four geomorphic units from west to east, including the Tibetan Plateau, the Inner Mongolia Plateau, Loess Plateau, and the North China Plain, with high terrain in the west and low terrain in the east. The average elevation in the western YRB is above 4000 m, with perennial snow and glacial landform development. The central region of the YRB is between 1000 and 2000 m above sea level, with loess landforms and severe soil erosion. The eastern YRB mainly consists of the alluvial plain of the Yellow River. The Yellow River Basin has a temperate monsoon climate, with an annual precipitation of 144–843 mm, and, in most places, it is 200–600 mm. Precipitation shows a pattern with more in the southeast and less in the northwest, and it gradually decreases from the southwest to the northeast. The YRB is an important energy, chemical, raw material, and general industrial base in northern China that has been facing an air pollution problem, primarily

from particulate matter, in recent years. According to the Chinese ecological environment status bulletin in 2019, of the top 20 cities with poor air quality in the country, 13 cities are located in the YRB, mainly in the central and eastern regions of the YRB and the North China Plain.

## 2.2. Data

We selected meteorological conditions and anthropogenic emissions as two types of influencing factors when conducting our analysis. The daily average meteorological data included six meteorological factors; these were accumulated precipitation (PRE, mm), surface air pressure (PRS, hPa), 2-meter relative humidity (RHU, %), sunshine duration (SSD, h), air temperature (TEM, °C) and 10-meter wind velocity (WIN, m/s). The anthropogenic emissions included five anthropogenic factors, namely, ammonia (NH<sub>3</sub>), nitrogen oxide (NO<sub>x</sub>), primary PM<sub>2.5</sub> (P\_PM), volatile organic compounds (VOC), and sulfur dioxide (SO<sub>2</sub>).

Daily average PM<sub>2.5</sub> concentrations (2015–2021) were derived from the National Environmental Monitoring Center, which included 104 city-monitoring sites in the YRB. Daily average meteorological monitoring data (2015–2017) were obtained from the China Meteorological Data Network (<http://data.cma.cn/> (accessed on 11 April 2022)) (Figures S1–S6 in the Supplementary Materials), which included 686 meteorological monitoring sites in the YRB. Anthropogenic emissions were derived from the Tsinghua University Emission Inventory (2015–2017) (MEIC, <http://meicmodel.org/> (accessed on 11 April 2022)) (Figures S7–S11 in the Supplementary Materials). The raster resolution of the inventory is 0.25° × 0.25°, and the temporal resolution includes the year and month [6,60].

## 2.3. GeoDetector Model

The GeoDetector model is a tool to detect and utilize spatial heterogeneity. This method has no linear assumption and has a clear physical meaning, which means that the multi-collinearity of input factors can be eliminated or ignored [61]. The GeoDetector model includes four detectors, comprising factor detection, interaction detection, risk area detection, and ecological detection. In our study, factor detection and interaction detection were used to quantify the effects of MC<sub>5</sub> and AEs and their interactions on PM<sub>2.5</sub> concentrations in the YRB.

Factor detectors can express the extent to which the independent variables explain the spatial differentiation of the dependent variables through  $q$ . In our study, the meteorological emission factors (PRE, PRS, RHU, SSD, TEM, and WIN) and anthropogenic emission precursors (NH<sub>3</sub>, NO<sub>x</sub>, P\_PM, SO<sub>2</sub>, and VOC) were selected as the independent variables (X), with PM<sub>2.5</sub> concentrations as the dependent variables (Y). The numerical variables were stratified and converted to categorical variables before implementing the variables. After comparing various classification methods, our study used the quantile method to classify each variable into 8 classes. These are expressed as:

$$q = 1 - \frac{\sum_{h=1}^L N_h \sigma_h^2}{N \sigma^2} = 1 - \frac{SSW}{SST} \quad (1)$$

$$SSW = \sum_{h=1}^L N_h \sigma_h^2 \quad (2)$$

$$SST = N \sigma^2 \quad (3)$$

The  $q$  value, which is between 0 and 1, represents the effect of the driving factor on spatial heterogeneity in PM<sub>2.5</sub> concentrations. If the spatial distribution of PM<sub>2.5</sub> concentrations is completely determined by a particular factor X, the  $q$ -value is 1; however, if there is no spatial correlation between PM<sub>2.5</sub> concentrations and factor X, then the  $q$ -value is 0. In the formula (1),  $h = 1 \dots$  and L represents the number of sub-regions of the influential factors;  $N$  and  $N_h$  are the numbers of the whole region and sub-regions in



classification  $h$ ;  $\sigma$  and  $\sigma_h$  represent the total variance and the variance of samples from sub-regions, respectively.

The interaction detector is used to identify the explanatory power of the interaction between any two influencing factors ( $X1 \cap X2$ ) on the dependent variable ( $Y$ ). We calculated the  $q$ -value of the interaction between any two factors ( $X1 \cap X2$ ) on  $Y$  and compared it with the  $q$ -values of  $X1$  and  $X2$ . The interaction between any two factors falls into five categories, comprising nonlinearly weakened, one-factor nonlinearly weakened, two-factor-enhanced, independent, and nonlinearly enhanced categories. For details, please refer to the literature [62].

### 3. Results

#### 3.1. Temporal Variation of PM2.5 Concentrations

Figure 2 shows the annual and seasonal variations in PM2.5 concentrations in the YRB from 2015 to 2021. From 2015 to 2021, the inter-annual variation of PM2.5 concentrations in the YRB demonstrates a decreasing trend, from 60  $\mu\text{g}/\text{m}^3$  in 2015 to 38  $\mu\text{g}/\text{m}^3$  in 2021. In terms of inter-season scale, the highest average PM2.5 concentrations occurred in winter, followed by spring and autumn, while the lowest PM2.5 concentrations occurred in summer. The highest PM2.5 concentrations occurred in winter 2017, at 97  $\mu\text{g}/\text{m}^3$ , and the lowest, at 21  $\mu\text{g}/\text{m}^3$ , in summer 2021. In general, the seasonal variation of PM2.5 concentrations in the YRB presents a fluctuating downward trend from 2015 to 2021. In addition, compared with other seasons, the trend in PM2.5 concentrations is more significant in winter.

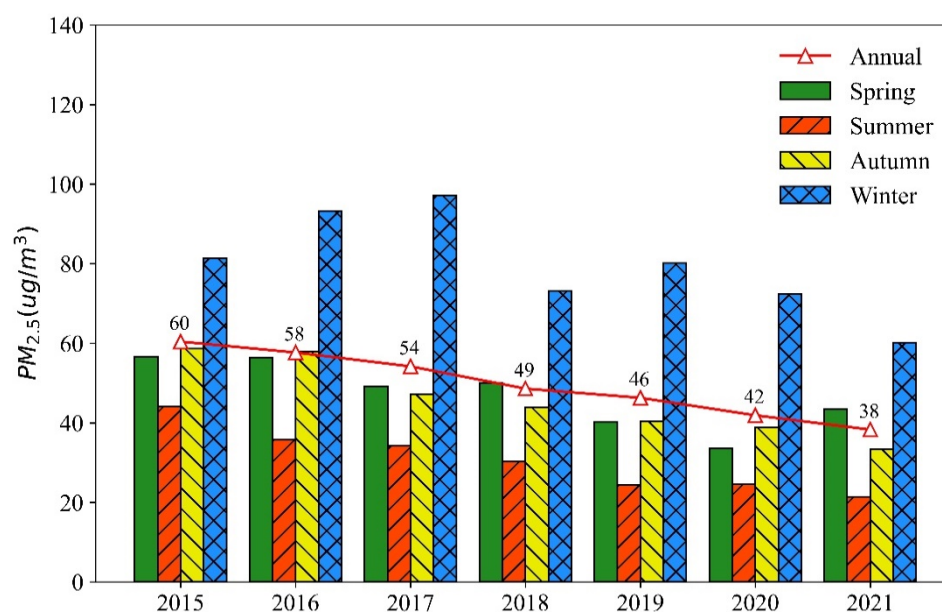


**Figure 2.** Inter-annual and inter-season variations of PM2.5 concentrations in the Yellow River Basin from 2015 to 2021.

Figure 3 shows the inter-month variation of PM2.5 concentrations in YRB from 2015 to 2021. The PM2.5 concentrations in the YRB display significant inter-month variation, with the lowest PM2.5 concentration value being 18  $\mu\text{g}/\text{m}^3$  in July 2021 and the highest PM2.5 concentration value being 115.9  $\mu\text{g}/\text{m}^3$  in December 2016. The inter-month variation of PM2.5 concentrations shows a sinusoidal pattern from 2015 to 2021, with a decreasing trend from January to May, a stable period from June to August, and an increasing trend from September to December. The fluctuation in monthly average PM2.5 concentrations from 2015 to 2021 demonstrates that the fluctuation range is the largest in January and December and the smallest in August. The kernel density curve shows that the curve for August is the steepest, with its peak corresponding to lower PM2.5 concentrations than other months, indicating that PM2.5 concentrations in major cities in the YRB are generally

lower in August. However, the kernel density curves in December and January are flatter and have the most peaks, indicating that PM<sub>2.5</sub> concentrations in major cities in the YRB are mostly high during this period, with a high degree of internal polarization.

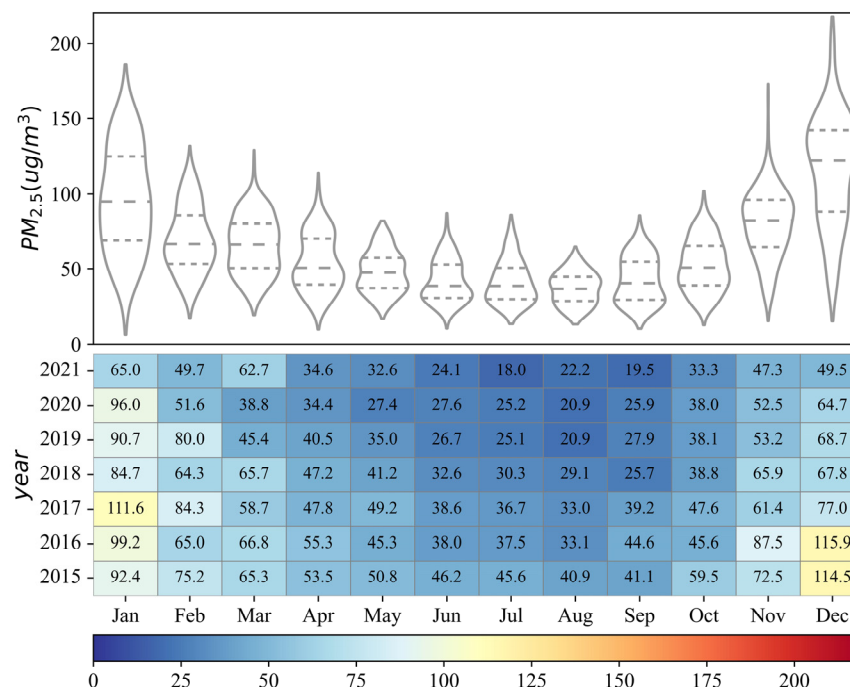


**Figure 3.** Inter-month variations of PM<sub>2.5</sub> concentrations in the Yellow River Basin from 2015 to 2021.

### 3.2. Spatial Variations of PM<sub>2.5</sub> Concentrations

The spatial distribution of the annual average PM<sub>2.5</sub> concentrations in the YRB from 2015 to 2021 is shown in Figure 4. There are obvious differences in the spatial distribution. From 2015 to 2021, the annual average PM<sub>2.5</sub> concentrations in the YRB display a significant downward trend. In 2015, the heavily polluted areas were mainly concentrated in the MYR and DYR areas, including the central and western parts of Shandong, most of Henan, the central part of Shaanxi, and Shanxi. The annual average PM<sub>2.5</sub> concentrations in these areas exceeded 50  $\mu\text{g}/\text{m}^3$ , far exceeding the China Ambient Air Quality Standard (CAAQS) Class II standard (35  $\mu\text{g}/\text{m}^3$ ). Low-pollution areas were mainly concentrated in the UYR, as well as in southwestern Shanxi and the western Shandong Peninsula. Compared to 2015, PM<sub>2.5</sub> concentrations levels decreased significantly in 2018, especially in the MYR and DYR areas. In 2018, high-pollution areas were concentrated in Henan, western Shandong, and central Shaanxi. In addition, relatively low pollution areas were mainly concentrated in western Shandong and southwest Shanxi. In 2021, PM<sub>2.5</sub> concentrations were further reduced; the relatively high-pollution areas at this point were mainly concentrated in Shanxi, Shaanxi, Henan, and Shandong.

### 3.3. Multi-Scale Effects of Influencing Factors on PM<sub>2.5</sub> Concentrations

At the whole-basin scale, the influence of driving factors on PM<sub>2.5</sub> concentrations demonstrates large inter-annual and inter-season variations (Figure 5 and Table S1 in the Supplementary Materials). MC<sub>S</sub> and AE<sub>S</sub> have similar inter-annual effects on PM<sub>2.5</sub> concentrations in YRB. PRS ( $q = 0.112$ ), TEM ( $q = 0.098$ ), and P\_PM ( $q = 0.083$ ) are thought to be the major influencing factors on PM<sub>2.5</sub> concentrations. PRS plays a dominant role among MC<sub>S</sub>, and P\_PM is the leading impactor among the AE<sub>S</sub>.

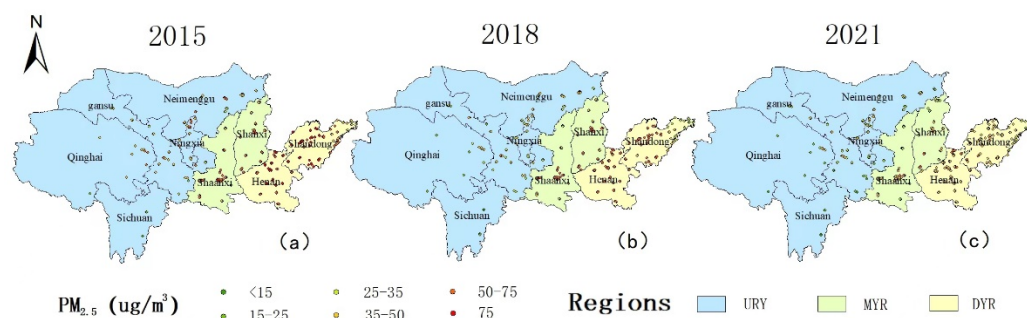


**Figure 4.** Spatial distribution of PM<sub>2.5</sub> annual average concentrations in the Yellow River Basin from 2015 to 2021 (a–c). (UYR denotes the Upper Yellow River Basin, MYR denotes the Middle Yellow River Basin, and DYR denotes the downstream area of the Yellow River Basin).

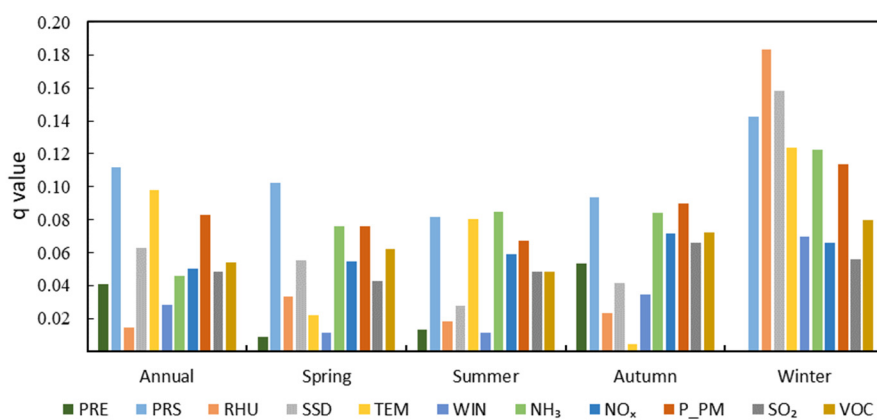


**Figure 5.** The inter-annual and inter-season  $q$ -values of the driving factors on PM<sub>2.5</sub> concentrations in the Yellow River Basin. (PRE denotes the accumulated precipitation; PRS denotes the surface air pressure; RHU denotes the 2-meter relative humidity; SSD denotes sunshine duration; TEM denotes air temperature; WIN denotes the 10-meter wind velocity; NH<sub>3</sub> denotes ammonia; NO<sub>x</sub> denotes nitrogen oxides; P\_PM denotes primary PM<sub>2.5</sub>; SO<sub>2</sub> denotes sulfur dioxide; VOC denotes volatile organic compounds).

In spring, the dominant factor affecting PM<sub>2.5</sub> concentrations in the YRB is PRS ( $q = 0.102$ ), followed by NH<sub>3</sub> ( $q = 0.076$ ) and P\_PM ( $q = 0.076$ ). In summer, NH<sub>3</sub> ( $q = 0.085$ ), PRS ( $q = 0.082$ ), and TEM ( $q = 0.080$ ) are the three dominant factors influencing PM<sub>2.5</sub> concentrations. In autumn, the dominant emission factors affecting PM<sub>2.5</sub> concentrations are PRS ( $q = 0.094$ ), P\_PM ( $q = 0.090$ ), and NH<sub>3</sub> ( $q = 0.084$ ). However, the dominant factors affecting PM<sub>2.5</sub> concentrations in winter are RHU ( $q = 0.184$ ), SSD ( $q = 0.158$ ), and PRS ( $q = 0.143$ ), respectively. In general, AE factors and MC<sub>S</sub> have a similar influence on PM<sub>2.5</sub> concentrations in spring, summer, and autumn, while MC<sub>S</sub> have a greater influence on PM<sub>2.5</sub> concentrations than AE<sub>S</sub> in winter.

Figure 6 and Table S2 in the Supplementary Materials show that MC<sub>S</sub> have a stronger inter-annual effect on PM<sub>2.5</sub> concentrations than AE<sub>S</sub> at the sub-basin scale, and TEM is the dominant influencing factor on PM<sub>2.5</sub> concentrations. In the UYR, TEM ( $q = 0.093$ ) is the dominant factor for PM<sub>2.5</sub> concentrations, followed by SO<sub>2</sub> ( $q = 0.052$ ) and P\_PM ( $q = 0.051$ ). In the MYR, TEM ( $q = 0.17$ ), SSD ( $q = 0.09$ ), and P\_PM ( $q = 0.06$ ) are the three dominant factors affecting PM<sub>2.5</sub> concentrations. However, the dominant factor affecting PM<sub>2.5</sub> concentrations is TEM ( $q = 0.15$ ), followed by WIN ( $q = 0.06$ ) and SSD ( $q = 0.06$ ) in the DYR. In general, TEM has similar inter-annual effects on the three sub-basins of the YRB, and the effect on PM<sub>2.5</sub> concentrations is the largest of all the influencing factors. However, P\_PM has a dominant inter-annual effect on PM<sub>2.5</sub> concentrations among the MC<sub>S</sub> in the three sub-basins.

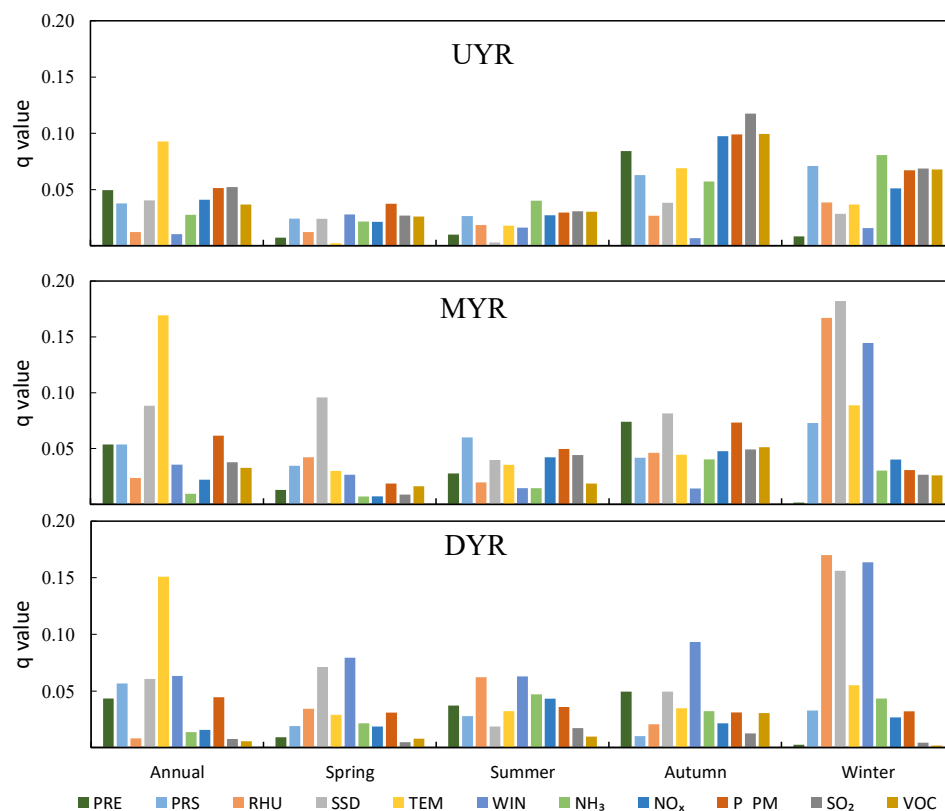


**Figure 6.** The inter-annual and inter-season  $q$ -values of the driving factors on PM<sub>2.5</sub> concentrations in the sub-basin of the Yellow River Basin. (UYR denotes the Upper Yellow River Basin; MYR, denotes the Middle Yellow River Basin; DYR, denotes the downstream area of the Yellow River Basin; PRE denotes accumulated precipitation; PRS denotes surface air pressure; RHU denotes 2-m relative humidity; SSD denotes sunshine duration; TEM denotes air temperature; WIN denotes 10-m wind velocity; NH<sub>3</sub> denotes ammonia; NO<sub>x</sub> denotes nitrogen oxides; P\_PM denotes primary PM<sub>2.5</sub>; SO<sub>2</sub> denotes sulfur dioxide; VOC denotes volatile organic compounds).

There are significant inter-season variations in the factors influencing PM<sub>2.5</sub> concentrations at the sub-basin scale (Figure 6 and Tables S3–S6 in the Supplementary Materials). In the UYR, MC<sub>S</sub> and AE<sub>S</sub> have a stronger influence on PM<sub>2.5</sub> in autumn and winter, compared to spring and summer. AE<sub>S</sub> have the greatest influence on PM<sub>2.5</sub> concentrations in autumn, ranked first by SO<sub>2</sub> ( $q = 0.12$ ), followed by VOC ( $q = 0.10$ ), P\_PM ( $q = 0.10$ ), and NO<sub>x</sub> ( $q = 0.10$ ). In the MYR, MC<sub>S</sub> and AE<sub>S</sub> have an equal influence on PM<sub>2.5</sub> concentrations in summer and autumn. However, MC<sub>S</sub> have a stronger effect compared to AE<sub>S</sub> on PM<sub>2.5</sub> concentrations in spring and winter, and MC<sub>S</sub> have the strongest effect on PM<sub>2.5</sub> in winter for all four seasons. In the DYR, MC<sub>S</sub> and AE<sub>S</sub> have similar effects on PM<sub>2.5</sub> concentrations in summer. However, MC<sub>S</sub> are the dominant factors regarding PM<sub>2.5</sub> concentrations in spring, autumn and winter, and MC<sub>S</sub> are the strongest in winter.

### 3.4. Multi-Scale Effects of Interactions on PM<sub>2.5</sub> Concentrations

We explored the effect of the interaction between 55 pairs of influencing factors on PM<sub>2.5</sub> concentrations, based on an interaction detector. The interaction between any two factors was analyzed by comparing the contribution of individual factors to PM<sub>2.5</sub> concentrations, with the integrated contribution being between the influencing factors. Figure 7 shows the interactive  $q$ -values and interaction types between the influencing factors at the whole-basin scale. The interactions of 23 pairs of influencing factors are two-factor-enhanced, while the remaining 32 pairs belong to non-linear enhancement. Among them, the interaction between PRS and TEM at the inter-annual scale ( $q = 0.23$ ) plays a dominant role in PM<sub>2.5</sub> concentrations, followed by PRE  $\cap$  SSD ( $q = 0.20$ ) and



TEM ∩ P\_PM ( $q = 0.20$ ). There is also a large seasonal difference in the interaction between potential influencing factors (Figure S12 in the Supplementary Materials). On a seasonal scale, the interaction between  $AE_S$  plays a dominant role in summer. In contrast, the interaction between  $MC_S$  plays a dominant role in PM2.5 concentrations in spring, autumn, and winter, with the strongest interaction between RHU and PRS in winter. There is also a significant influence between  $MC_S$  and  $AE_S$ , with the strongest interaction shown between RHU and P\_PM and  $NH_3$  in winter ( $q = 0.27$ ).

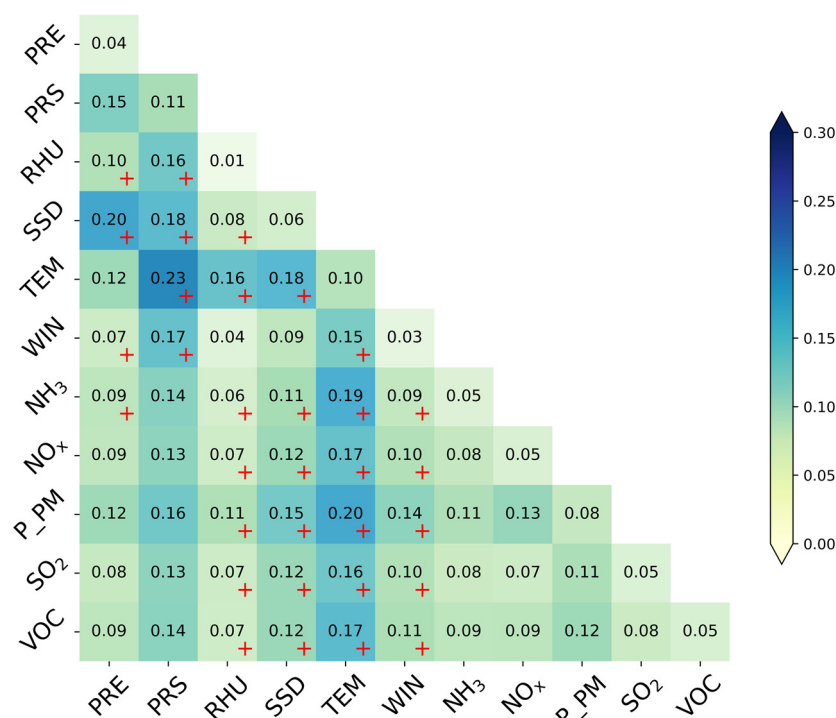


**Figure 7.** The inter-annual interaction in the factors influences the spatial pattern of PM2.5 concentrations in the Yellow River Basin. Note: “+” means that the type of interaction belongs to nonlinear enhancement; otherwise, it belongs to bivariate enhancement. (PRE denotes accumulated precipitation; PRS denotes surface air pressure; RHU denotes 2-m relative humidity; SSD denotes sunshine duration; TEM denotes air temperature; WIN denotes 10-m wind velocity; NH<sub>3</sub> denotes ammonia; NO<sub>x</sub> denotes nitrogen oxides; P\_PM denotes primary PM2.5; SO<sub>2</sub> denotes sulfur dioxide; VOC denotes volatile organic compounds).

Figures S13–S18 in the Supplementary Materials show the significant regional variations in the interactions at the sub-basin scale. In the UYR, the inter-annual interactions between  $MC_S$  have a similar effect as those between  $MC_S$  and  $AE_S$ . In the MYR, the inter-annual interactions between  $MC_S$  play a dominant role in PM2.5 concentrations, with the strongest interactions occurring between TEM and SSD. Similar to MYR, the inter-annual interaction between  $MC_S$  plays a dominant role in terms of PM2.5 concentrations in the DYR region, with the strongest interactions between TEM and WIN. In addition, Figures S13–S18 also show the  $q$ -values of the inter-season interaction between the impact factors in the sub-basin, indicating that there is also significant inter-season variation in the interaction between the impact factors in the sub-basin.

#### 4. Discussion

The inter-annual PM2.5 concentrations in the YRB displayed a steady downward trend from 2015 to 2021, which is consistent with a series of atmospheric pollution control policies that China has implemented in recent years. For example, the Chinese government promulgated the Air Pollution Prevention and Control Action Plan in 2013 and the Three-Year Action Plan to Win the Blue Sky Defense War in 2018. The imple-

mentation of these air-quality policies has had a significant effect on reducing PM<sub>2.5</sub> concentrations [10,11,63,64]. The inter-season variation of PM<sub>2.5</sub> concentrations in the YRB shows a fluctuating downward trend, and the trend of PM<sub>2.5</sub> concentrations in winter is more obvious. At the inter-month scale, PM<sub>2.5</sub> concentrations demonstrate a U-shaped distribution from January to December, with January and December at the peak and June to August at the bottom of the curve, which is consistent with previous studies [56,65]. In terms of spatial distribution, PM<sub>2.5</sub> concentrations in the YRB display a spatial distribution pattern that is high in the east and low in the west. The high PM<sub>2.5</sub> concentrations are mainly concentrated in Henan, Shandong, Shanxi, and Shaanxi, and are located in the MYR and DYR. This may be due to the dense population in the region; the related industries are mainly for energy and basic raw materials, and the energy consumption structure is mainly with coal [30,66,67].

We quantified the multi-scale effects of MC<sub>S</sub> and AE<sub>S</sub> and their interactions on PM<sub>2.5</sub> concentrations in the YRB, based on a GeoDetector model. We found that there are significant inter-annual and inter-season variations in the effects of MC<sub>S</sub> and AE<sub>S</sub> on PM<sub>2.5</sub> concentrations at the whole-basin scale. The inter-annual effects of MC<sub>S</sub> and AE<sub>S</sub> on PM<sub>2.5</sub> concentrations are similar, and PRS and TEM are the two main factors affecting PM<sub>2.5</sub> concentrations. TEM and PRS influence particulate matter transport and accumulation by affecting convection [21]. Air pressure is positively correlated with PM<sub>2.5</sub> concentrations [14]. Air pressure affects the dispersion and accumulation of PM<sub>2.5</sub> by creating low-level wind convergence. High-pressure systems can lead to environmental stagnation, which affects PM<sub>2.5</sub> transport and is detrimental to PM<sub>2.5</sub> dispersion [68]. Comparing relevant studies in other regions of China, previous scholars have found that air pressure also has a dominant effect on PM<sub>2.5</sub> concentrations in Tibet and China [69,70].

A strong relationship between temperature and PM<sub>2.5</sub> concentrations has been demonstrated in the literature [3,14,15,71]. Strong thermal activity, such as turbulence, at high temperatures will accelerate the dispersion of PM<sub>2.5</sub> [72]. In contrast, a low temperature reduces atmospheric convection and enhances PM<sub>2.5</sub> agglomeration. In general, temperatures decrease as altitude increases, and temperature inversion occurs when temperatures increase with altitude [73]. Temperature inversion weakens PM<sub>2.5</sub> scattering and dispersion, resulting in higher local PM<sub>2.5</sub> concentrations [3,74,75]. Comparing relevant studies in other regions of China, some scholars found that temperature also has a dominant effect on PM<sub>2.5</sub> concentrations in regions such as the Yangtze River delta [76], Pearl River delta [77], and northeast China [78]. In winter, however, MC<sub>S</sub> play the dominant role and RHU is the most important factor, which is consistent with the results from previous studies. One possible reason is that aqueous-phase aerosol chemistry drives secondary pollution [79–82]. The finding of RHU as the dominant influencing factor of PM<sub>2.5</sub> concentrations has also been verified in relevant studies on the Beijing-Tianjin-Hebei region [83], the Yangtze River delta [40], and the Pearl River delta [84] in China.

We found that there are spatial and seasonal variations in the effects of anthropogenic and meteorological factors on PM<sub>2.5</sub> concentrations in the sub-basins. MC<sub>S</sub> have a stronger inter-annual influence on PM<sub>2.5</sub> concentrations than AE<sub>S</sub> in the sub-basins. TEM is the dominant influencing factor in each sub-basin, which is consistent with previous studies [39,58,59]. On the inter-season scale, MC<sub>S</sub> play a dominant role in winter in the MYR and UYR, which is different from previous studies. In northern China the influence of AE<sub>S</sub> on PM<sub>2.5</sub> concentrations in winter has been found to be greater than MC<sub>S</sub>, which is due to high coal consumption and high industrial and vehicular emissions during the heating period, resulting in severe regional PM<sub>2.5</sub> pollution. The Fenwei Plain is located in the MYR, and PM<sub>2.5</sub> pollution is severe in this region. PM<sub>2.5</sub> concentrations that are attributable to vehicle exhaust, biomass combustion, substances from coal combustion, and dust have been reported in previous studies [51,85]. WIN has a significant effect on PM<sub>2.5</sub> concentrations in the four seasons of the DYR, with the strongest effects in winter, which finding is also consistent with previous studies [53,58,86]. Some major cities in the DYR are located in the Beijing-Tianjin-Hebei atmospheric pollution transport channel, in

which wind speed affects PM<sub>2.5</sub> transmission across the region. As a result, the formation of heavy PM<sub>2.5</sub> pollution is driven by lower wind speeds in winter in the region. Related studies have confirmed that at low wind speeds, increasing wind speed may lead to less turbulence intensity, weak horizontal atmospheric motion, and a dominant subsidence motion in the upper air, which creates unfavorable dispersion conditions for PM<sub>2.5</sub> [87–90].

Compared with other anthropogenic emissions, P<sub>PM</sub> has significant effects on PM<sub>2.5</sub> concentrations at whole-basin and sub-basin scales. In recent years, anthropogenic emissions in the YRB have shown a decreasing trend over the years, indicating that reducing anthropogenic emissions can effectively reduce P<sub>PM</sub> emissions, while pollution control measures are effective in reducing PM<sub>2.5</sub> pollution. We find that NH<sub>3</sub> is the dominant factor regarding PM<sub>2.5</sub> in the YRB in summer. NH<sub>3</sub>, as an alkaline gas, has an important influence on the formation of PM<sub>2.5</sub>, as has been demonstrated in China and elsewhere in the world [91–93]. Agricultural activities, as well as relatively high temperatures, result in peak agricultural ammonia emissions in summer. Henan and Shandong in the DYR are both important agricultural provinces with much higher agricultural NH<sub>3</sub> emissions than other regions [10,94,95]. Among all anthropogenic ammonia emission sources in Henan Province, livestock and nitrogen fertilizer are the main sources of total NH<sub>3</sub> emissions, with an average share of about 46.5% and 42.9% [96]. Previous studies have demonstrated that the mitigation of agricultural ammonia emissions can help reduce PM<sub>2.5</sub> pollution [24], and ammonia emission reduction is more cost-effective than NO<sub>x</sub> emission reduction [52]. Compared with MC<sub>S</sub>, AEs are more controllable. Therefore, we should focus on the corresponding policies for ammonia emission reduction in the future, which is important for the effective mitigation of PM<sub>2.5</sub> pollution.

The interaction detector showed that the types of interactions between the influencing factors mainly included non-linear enhancement and bivariate enhancement, with non-linear enhancement dominating, indicating that interactions between factors had a significant enhancing effect on PM<sub>2.5</sub> concentrations. In the whole basin and sub-basin, the interaction between NH<sub>3</sub> and anthropogenic emissions have a dominant effect on PM<sub>2.5</sub> concentrations in summer, which may be due to the accelerated chemical reactions between NH<sub>3</sub> and other anthropogenic emissions under higher temperature conditions, which have an impact on PM<sub>2.5</sub> concentrations [97,98]. At the whole-basin scale, the interaction between MC<sub>S</sub> plays a dominant role in winter (RHU ∩ PRS), which may be due to secondary pollution driven by aqueous-phase aerosol chemistry in the YRB in winter [79,80]. Meanwhile, low pressure is often accompanied by low wind speed and higher domestic heating emissions in winter in the YRB, which together accelerate the rapid accumulation of PM<sub>2.5</sub> [73,87,99,100].

There are some limitations to our study at present since it is limited by data accessibility; we used PM<sub>2.5</sub> site monitoring data from 2015 to 2021 and meteorological conditions and emission inventory data from 2015 to 2017, which could conduce some uncertainty in the results. In the future, we will update meteorological conditions and emission inventory data to be consistent with PM<sub>2.5</sub> concentrations. In the future, we will also focus on evaluating the effectiveness of air pollution policies and the impact of the implementation of air pollution policies on PM<sub>2.5</sub> concentrations in the YRB in recent years. Relevant studies have demonstrated that PM<sub>2.5</sub> reduction may lead to an ozone increase, which will bring uncertainty regarding the effectiveness of policy implementation. Therefore, we will combine PM<sub>2.5</sub> with ozone measurements to conduct research on their synergistic management, in order to provide insight into the future development of precise air pollution prevention and control policies.

## 5. Conclusions

We analyzed the multi-scale variations of PM<sub>2.5</sub> concentrations in the YRB and elucidated the multi-scale effects of meteorological conditions and anthropogenic emissions, as well as their interactions, on PM<sub>2.5</sub> concentrations in the YRB. The results contribute to a better understanding of the driving mechanisms of PM<sub>2.5</sub> concentrations in the YRB

and provide insight into the future development of regional air pollution policies. We verified that the PM<sub>2.5</sub> concentrations in the YRB displayed significant spatial and temporal variations from 2015 to 2021. The inter-annual variation of PM<sub>2.5</sub> concentrations in the YRB from 2015 to 2021 displays a steadily decreasing trend. The PM<sub>2.5</sub> concentrations in terms of inter-season scale show a fluctuating decreasing trend, and the variation is more obvious in winter. The PM<sub>2.5</sub> inter-month concentrations display a sinusoidal pattern from 2015 to 2021, with January and December at the peak and June to August at the bottom. The PM<sub>2.5</sub> concentrations in the YRB demonstrate a spatial distribution pattern that is high in the east and low in the west, while the high PM<sub>2.5</sub> concentrations are mainly concentrated in the MYR and DYR.

MCs and AEs have similar inter-annual effects on PM<sub>2.5</sub> concentrations across the whole basin, with PRS and TEM being the two most dominant factors. In contrast, MCs play a dominant role in winter, and RHU is the most important factor. At the sub-basin scale, MCs have stronger inter-annual effects on PM<sub>2.5</sub> concentrations than AEs, while TEM is the dominant impact factor. Wind speed has a significant effect on PM<sub>2.5</sub> concentrations across all four seasons in the DYR and has the strongest effect in winter. P<sub>PM</sub> and NH<sub>3</sub> are the two main anthropogenic emission factors affecting PM<sub>2.5</sub> concentrations. The interaction between NH<sub>3</sub> and other anthropogenic emissions plays a dominant role in PM<sub>2.5</sub> concentrations at the whole-basin and sub-basin scales in summer, while the interaction between meteorological factors (RHU  $\cap$  PRS) plays a dominant role at the whole-basin scale in winter.

This study can provide a policy reference for the mitigation of PM<sub>2.5</sub> pollution. The influence of atmospheric processes on PM<sub>2.5</sub> concentrations is complex. We found that MCs such as PRS, TEM, WIN, and RHU have important effects on PM<sub>2.5</sub> concentrations in the Yellow River Basin. It is important to formulate a reasonable spatial planning policy for green spaces, establish and improve ecological landscapes and conservation corridors, utilize artificial precipitation enhancement, and build urban ventilation corridors to reduce regional PM<sub>2.5</sub> concentrations [101].

Among the AEs, the influence of P<sub>PM</sub> and NH<sub>3</sub> on PM<sub>2.5</sub> concentrations in the Yellow River Basin is more obvious. Primary PM<sub>2.5</sub> and secondary PM<sub>2.5</sub> have different pathways of formation; controlling primary PM<sub>2.5</sub> emissions is effective in mitigating PM<sub>2.5</sub> pollution. Therefore, in the future, it will be necessary to strengthen the regulation of emission reduction measures, strengthen the management of vehicle emission control policies, promote the optimization and adjustment of high energy-consuming and high-polluting industries, adjust the energy consumption structure, and optimize industrial processes in the Yellow River Basin to reduce the emissions of primary particulate matter. In the case of ammonia, it is necessary to target agricultural ammonia sources to reduce emissions, optimize farm management patterns, improve fertilizer quality, improve fertilizer application techniques and increase fertilizer utilization efficiency. In addition, more attention should be paid to non-agricultural sources of ammonia emissions, and the model of combining cultivation and farming is the key to ammonia reduction in farming.

**Supplementary Materials:** The following supporting information can be downloaded at: <https://www.mdpi.com/article/10.3390/ijerph192215060/s1>.

**Author Contributions:** Conceptualization, P.L.; methodology, P.L. and H.S.; software, J.Z. and L.Z. and Y.Z.; validation, P.L. and H.S.; formal analysis, J.Z. and J.Y.; investigation, P.L. and J.Z.; resources, H.S. and J.D.; data curation, P.L.; writing—original draft preparation, J.Z.; writing—review and editing, P.L.; visualization, L.Z. and Y.L. and B.L.; supervision, P.L. and C.M. All authors have read and agreed to the published version of the manuscript.

**Funding:** This research was funded by the Natural Science Foundation of China (42101424) and by the Natural Science Foundation of Henan (No. 202300410076).

**Institutional Review Board Statement:** The studies not involving humans or animals. So ethical review and approval were not applicable for this study.

**Acknowledgments:** This research was funded by the Natural Science Foundation of China (42101424) and by the Natural Science Foundation of Henan (No. 202300410076).

**Conflicts of Interest:** The authors declare no conflict of interest.

## Abbreviations

AEs: anthropogenic emissions; CO, carbon monoxide; MCs, meteorological conditions; PM<sub>2.5</sub>, fine particulate matter; NH<sub>3</sub>, ammonia; NO<sub>x</sub>, nitrogen oxides; P<sub>PM</sub>, primary PM<sub>2.5</sub>; PRE, accumulated precipitation; PRS, surface air pressure; RHU, 2-meter relative humidity; SO<sub>2</sub>, sulfur dioxide; SSD, sunshine duration; TEM, air temperature; VOC, volatile organic compounds; WIN, 10-m wind velocity; YRB, the Yellow River Basin; UYR, the Upper Yellow River Basin; MYR, the Middle Yellow River Basin; DYR, the downstream area of the Yellow River Basin.

## References

- Huang, R.J.; Zhang, Y.; Bozzetti, C.; Ho, K.F.; Cao, J.J.; Han, Y.; Daellenbach, K.R.; Slowik, J.G.; Platt, S.M.; Canonaco, F.; et al. High Secondary Aerosol Contribution to Particulate Pollution during Haze Events in China. *Nature* **2015**, *514*, 218–222. [[CrossRef](#)] [[PubMed](#)]
- Li, K.; Jacob, D.J.; Liao, H.; Zhu, J.; Shah, V.; Shen, L.; Bates, K.H.; Zhang, Q.; Zhai, S. A Two-Pollutant Strategy for Improving Ozone and Particulate Air Quality in China. *Nat. Geosci.* **2019**, *12*, 906–910. [[CrossRef](#)]
- Jing, Z.; Liu, P.; Wang, T.; Song, H.; Lee, J.; Xu, T.; Xing, Y. Effects of Meteorological Factors and Anthropogenic Precursors on PM<sub>2.5</sub> Concentrations in Cities in China. *Sustainability* **2020**, *12*, 3550. [[CrossRef](#)]
- Chen, L.; Zhu, J.; Liao, H.; Yang, Y.; Yue, X. Meteorological Influences on PM<sub>2.5</sub> and O<sub>3</sub> Trends and Associated Health Burden since China's Clean Air Actions. *Sci. Total Environ.* **2020**, *744*, 140837. [[CrossRef](#)] [[PubMed](#)]
- Lelieveld, J.; Evans, J.S.; Fnais, M.; Giannadaki, D.; Pozzer, A. The Contribution of Outdoor Air Pollution Sources to Premature Mortality on a Global Scale. *Nature* **2015**, *525*, 367–371. [[CrossRef](#)] [[PubMed](#)]
- Liu, J.; Rühland, K.M.; Chen, J.; Xu, Y.; Chen, S.; Chen, Q.; Huang, W.; Xu, Q.; Chen, F.; Smol, J.P. Aerosol-Weakened Summer Monsoons Decrease Lake Fertilization on the Chinese Loess Plateau. *Nat. Clim. Chang.* **2017**, *7*, 190–194. [[CrossRef](#)]
- Song, C.; He, J.; Wu, L.; Jin, T.; Chen, X.; Li, R.; Ren, P.; Zhang, L.; Mao, H. Health Burden Attributable to Ambient PM<sub>2.5</sub> in China. *Environ. Pollut.* **2017**, *223*, 575–586. [[CrossRef](#)]
- He, W.; Meng, H.; Han, J.; Zhou, G.; Zheng, H.; Zhang, S. Spatiotemporal PM<sub>2.5</sub> estimations in China from 2015 to 2020 using an improved gradient boosting decision tree. *Chemosphere* **2022**, *296*, 134003. [[CrossRef](#)]
- Patz, J.A.; Campbell-Lendrum, D.; Holloway, T.; Foley, J.A. Impact of Regional Climate Change on Human Health. *Nature* **2005**, *438*, 310–317. [[CrossRef](#)]
- Geng, G.; Xiao, Q.; Zheng, Y.; Tong, D.; Zhang, Y.; Zhang, X.; Zhang, Q.; He, K.; Liu, Y. Impact of China's Air Pollution Prevention and Control Action Plan on PM<sub>2.5</sub> Chemical Composition over Eastern China. *Sci. China Earth Sci.* **2019**, *62*, 1872–1884. [[CrossRef](#)]
- Zhang, Q.; Zheng, Y.; Tong, D.; Shao, M.; Wang, S.; Zhang, Y.; Xu, X.; Wang, J.; He, H.; Liu, W.; et al. Drivers of Improved PM<sub>2.5</sub> Air Quality in China from 2013 to 2017. *Proc. Natl. Acad. Sci. USA* **2019**, *116*, 24463–24469. [[CrossRef](#)] [[PubMed](#)]
- Chen, Z.; Chen, D.; Wen, W.; Zhuang, Y.; Kwan, M.P.; Chen, B.; Zhao, B.; Yang, L.; Gao, B.; Li, R.; et al. Evaluating the “2+26” Regional Strategy for Air Quality Improvement during Two Air Pollution Alerts in Beijing: Variations in PM<sub>2.5</sub> Concentrations, Source Apportionment, and the Relative Contribution of Local Emission and Regional Transport. *Atmos. Chem. Phys.* **2019**, *19*, 6879–6891. [[CrossRef](#)]
- Li, J.; Chen, H.; Li, Z.; Wang, P.; Cribb, M.; Fan, X. Low-Level Temperature Inversions and Their Effect on Aerosol Condensation Nuclei Concentrations under Different Large-Scale Synoptic Circulations. *Adv. Atmos. Sci.* **2015**, *32*, 898–908. [[CrossRef](#)]
- Li, X.; Song, H.; Zhai, S.; Lu, S.; Kong, Y.; Xia, H.; Zhao, H. Particulate Matter Pollution in Chinese Cities: Areal-Temporal Variations and Their Relationships with Meteorological Conditions (2015–2017). *Environ. Pollut.* **2019**, *246*, 11–18. [[CrossRef](#)]
- Megaritis, A.G.; Fountoukis, C.; Charalampidis, P.E.; Denier Van Der Gon, H.A.C.; Pilinis, C.; Pandis, S.N. Linking Climate and Air Quality over Europe: Effects of Meteorology on PM<sub>2.5</sub> concentrations. *Atmos. Chem. Phys.* **2014**, *14*, 10283–10298. [[CrossRef](#)]
- Qu, L.; Liu, S.; Ma, L.; Zhang, Z.; Du, J.; Zhou, Y.; Meng, F. Evaluating the Meteorological Normalized PM<sub>2.5</sub> Trend (2014–2019) in the “2+26” Region of China Using an Ensemble Learning Technique. *Environ. Pollut.* **2020**, *266*, 115346. [[CrossRef](#)]
- Dawson, J.P.; Adams, P.J.; Pandis, S.N. Sensitivity of PM<sub>2.5</sub> to Climate in the Eastern US: A Modeling Case Study. *Atmos. Chem. Phys.* **2007**, *7*, 4295–4309. [[CrossRef](#)]
- Liu, Y.; Zhang, T.; Liu, Q.; Zhang, R.; Sun, Z.; Zhang, M. Seasonal Variation of Physical and Chemical Properties in TSP, PM<sub>10</sub> and PM<sub>2.5</sub> at a Roadside Site in Beijing and Their Influence on Atmospheric Visibility. *Aerosol Air Qual. Res.* **2014**, *14*, 954–969. [[CrossRef](#)]
- Zhang, Q.; Ma, Q.; Zhao, B.; Liu, X.; Wang, Y.; Jia, B.; Zhang, X. Winter Haze over North China Plain from 2009 to 2016: Influence of Emission and Meteorology. *Environ. Pollut.* **2018**, *242*, 1308–1318. [[CrossRef](#)]



20. Liu, Q.; Wang, S.; Zhang, W.; Li, J.; Dong, G. The Effect of Natural and Anthropogenic Factors on PM<sub>2.5</sub>: Empirical Evidence from Chinese Cities with Different Income Levels. *Sci. Total Environ.* **2019**, *653*, 157–167. [[CrossRef](#)]
21. Li, Y.; Chen, Q.; Zhao, H.; Wang, L.; Tao, R. Variations in Pm<sub>10</sub>, Pm<sub>2.5</sub> and Pm<sub>1.0</sub> in an Urban Area of the Sichuan Basin and Their Relation to Meteorological Factors. *Atmosphere* **2015**, *6*, 150–163. [[CrossRef](#)]
22. Wang, C.; An, X.; Zhang, P.; Sun, Z.; Cui, M.; Ma, L. Comparing the Impact of Strong and Weak East Asian Winter Monsoon on PM<sub>2.5</sub> Concentration in Beijing. *Atmos. Res.* **2019**, *215*, 165–177. [[CrossRef](#)]
23. Wang, Z.; Zhong, S.; Peng, Z.R.; Cai, M. Fine-Scale Variations in PM<sub>2.5</sub> and Black Carbon Concentrations and Corresponding Influential Factors at an Urban Road Intersection. *Build. Environ.* **2018**, *141*, 215–225. [[CrossRef](#)]
24. Ye, Z.; Guo, X.; Cheng, L.; Cheng, S.; Chen, D.; Wang, W.; Liu, B. Reducing PM<sub>2.5</sub> and Secondary Inorganic Aerosols by Agricultural Ammonia Emission Mitigation within the Beijing-Tianjin-Hebei Region, China. *Atmos. Environ.* **2019**, *219*, 116989. [[CrossRef](#)]
25. Yang, J.; Liu, P.; Song, H.; Miao, C.; Wang, F.; Xing, Y.; Wang, W.; Liu, X.; Zhao, M. Effects of Anthropogenic Emissions from Different Sectors on PM<sub>2.5</sub> Concentrations in Chinese Cities. *Int. J. Environ. Res. Public Health* **2021**, *18*, 10869. [[CrossRef](#)] [[PubMed](#)]
26. Wang, Y.; Li, X.; Wang, Q.; Zhou, B.; Liu, S.; Tian, J.; Hao, Q.; Li, G.; Han, Y.; Hang Ho, S.S.; et al. Response of Aerosol Composition to the Clean Air Actions in Baoji City of Fen-Wei River Basin. *Environ. Res.* **2022**, *210*, 112936. [[CrossRef](#)]
27. Li, G.; Fang, C.; Wang, S.; Sun, S. The Effect of Economic Growth, Urbanization, and Industrialization on Fine Particulate Matter (PM<sub>2.5</sub>) Concentrations in China. *Environ. Sci. Technol.* **2016**, *50*, 11452–11459. [[CrossRef](#)]
28. Wang, X.; Tian, G.; Yang, D.; Zhang, W.; Lu, D.; Liu, Z. Responses of PM<sub>2.5</sub> Pollution to Urbanization in China. *Energy Policy* **2018**, *123*, 602–610. [[CrossRef](#)]
29. Li, C.; Wang, Z.; Li, B.; Peng, Z.R.; Fu, Q. Investigating the Relationship between Air Pollution Variation and Urban Form. *Build. Environ.* **2019**, *147*, 559–568. [[CrossRef](#)]
30. Li, F.; Zhou, T. Effects of Urban Form on Air Quality in China: An Analysis Based on the Spatial Autoregressive Model. *Cities* **2019**, *89*, 130–140. [[CrossRef](#)]
31. McCarty, J.; Kaza, N. Urban Form and Air Quality in the United States. *Landsc. Urban Plan.* **2015**, *139*, 168–179. [[CrossRef](#)]
32. She, Q.; Peng, X.; Xu, Q.; Long, L.; Wei, N.; Liu, M.; Jia, W.; Zhou, T.; Han, J.; Xiang, W.; et al. Air Quality and Its Response to Satellite-Derived Urban Form in the Yangtze River Delta, China. *Ecol. Indic.* **2017**, *75*, 297–306. [[CrossRef](#)]
33. Yang, H.; Liu, J.; Jiang, K.; Meng, J.; Guan, D.; Xu, Y.; Tao, S. Multi-Objective Analysis of the Co-Mitigation of CO<sub>2</sub> and PM<sub>2.5</sub> Pollution by China's Iron and Steel Industry. *J. Clean. Prod.* **2018**, *185*, 331–341. [[CrossRef](#)]
34. Yang, H.; Tao, W.; Liu, Y.; Qiu, M.; Liu, J.; Jiang, K.; Yi, K.; Xiao, Y.; Tao, S. The Contribution of the Beijing, Tianjin and Hebei Region's Iron and Steel Industry to Local Air Pollution in Winter. *Environ. Pollut.* **2019**, *245*, 1095–1106. [[CrossRef](#)] [[PubMed](#)]
35. Wang, Y.; Liu, C.G.; Wang, Q.; Qin, Q.; Ren, H.; Cao, J. Impacts of Natural and Socioeconomic Factors on PM<sub>2.5</sub> from 2014 to 2017. *J. Environ. Manag.* **2021**, *284*, 112071. [[CrossRef](#)]
36. Yang, Q.; Yuan, Q.; Li, T.; Shen, H.; Zhang, L. The Relationships between PM<sub>2.5</sub> and Meteorological Factors in China: Seasonal and Regional Variations. *Int. J. Environ. Res. Public Health* **2017**, *14*, 1510. [[CrossRef](#)]
37. Dong, J.; Liu, P.; Song, H.; Yang, D.; Yang, J.; Song, G.; Miao, C.; Zhang, J.; Zhang, L. Effects of anthropogenic precursor emissions and meteorological conditions on PM<sub>2.5</sub> concentrations over the “2+26” cities of northern China. *Environ. Pollut.* **2022**, *315*, 120392. [[CrossRef](#)]
38. Shi, P.; Zhang, G.; Kong, F.; Chen, D.; Azorin-Molina, C.; Guijarro, J.A. Variability of Winter Haze over the Beijing-Tianjin-Hebei Region Tied to Wind Speed in the Lower Troposphere and Particulate Sources. *Atmos. Res.* **2019**, *215*, 1–11. [[CrossRef](#)]
39. Liu, J.; Mauzerall, D.L.; Chen, Q.; Zhang, Q.; Song, Y.; Peng, W.; Klimont, Z.; Qiu, X.; Zhang, S.; Hu, M.; et al. Air Pollutant Emissions from Chinese Households: A Major and Underappreciated Ambient Pollution Source. *Proc. Natl. Acad. Sci. USA* **2016**, *113*, 7756–7761. [[CrossRef](#)]
40. Li, L.; Huang, C.; Huang, H.Y.; Wang, Y.J.; Yan, R.S.; Zhang, G.F.; Zhou, M.; Lou, S.R.; Tao, S.K.; Wang, H.L.; et al. An Integrated Process Rate Analysis of a Regional Fine Particulate Matter Episode over Yangtze River Delta in 2010. *Atmos. Environ.* **2014**, *91*, 60–70. [[CrossRef](#)]
41. Lu, D.; Mao, W.; Yang, D.; Zhao, J.; Xu, J. Effects of Land-Use and Landscape Pattern on PM<sub>2.5</sub> in Yangtze River Delta in China. *Atmos. Pollut. Res.* **2018**, *9*, 705–713. [[CrossRef](#)]
42. Ma, T.; Duan, F.; He, K.; Qin, Y.; Tong, D.; Geng, G.; Liu, X.; Li, H.; Yang, S.; Ye, S.; et al. Air Pollution Characteristics and Their Relationship with Emissions and Meteorology in the Yangtze River Delta Region during 2014–2016. *J. Environ. Sci.* **2019**, *83*, 8–20. [[CrossRef](#)] [[PubMed](#)]
43. Xu, G.; Ren, X.; Xiong, K.; Li, L.; Bi, X.; Wu, Q. Analysis of the Driving Factors of PM<sub>2.5</sub> Concentration in the Air: A Case Study of the Yangtze River Delta, China. *Ecol. Indic.* **2020**, *110*, 105889. [[CrossRef](#)]
44. Huang, H.; Ho, K.F.; Lee, S.C.; Tsang, P.K.; Ho, S.S.H.; Zou, C.W.; Zou, S.C.; Cao, J.J.; Xu, H.M. Characteristics of Carbonaceous Aerosol in PM<sub>2.5</sub>: Pearl Delta River Region, China. *Atmos. Res.* **2012**, *104*, 227–236. [[CrossRef](#)]
45. Wang, W.; Ren, L.; Zhang, Y.; Chen, J.; Liu, H.; Bao, L.; Fan, S.; Tang, D. Aircraft Measurements of Gaseous Pollutants and Particulate Matter over Pearl River Delta in China. *Atmos. Environ.* **2008**, *42*, 6187–6202. [[CrossRef](#)]
46. Yin, S.; Huang, Z.; Zheng, J.; Huang, X.; Chen, D.; Tan, H. Characteristics of Inorganic Aerosol Formation over Ammonia-Poor and Ammonia-Rich Areas in the Pearl River Delta Region, China. *Atmos. Environ.* **2018**, *177*, 120–131. [[CrossRef](#)]

47. Zhao, X.; Wang, X.; Ding, X.; He, Q.; Zhang, Z.; Liu, T.; Fu, X.; Gao, B.; Wang, Y.; Zhang, Y.; et al. Compositions and Sources of Organic Acids in Fine Particles (PM<sub>2.5</sub>) over the Pearl River Delta Region, South China. *J. Environ. Sci.* **2014**, *26*, 110–121. [[CrossRef](#)]
48. Liu, Y.; Shi, G.; Zhan, Y.; Zhou, L.; Yang, F. Characteristics of PM<sub>2.5</sub> Spatial Distribution and Influencing Meteorological Conditions in Sichuan Basin, Southwestern China. *Atmos. Environ.* **2021**, *253*, 118364. [[CrossRef](#)]
49. Liu, Y.; Yue, W.; Fan, P.; Zhang, Z.; Huang, J. Assessing the Urban Environmental Quality of Mountainous Cities: A Case Study in Chongqing, China. *Ecol. Indic.* **2017**, *81*, 132–145. [[CrossRef](#)]
50. Zheng, Y.; Wang, X.; Zhang, X.; Hu, G. Multi-Spatiotemporal Patterns of Aerosol Optical Depth and Influencing Factors during 2000–2020 from Two Spatial Perspectives: The Entire Yellow River Basin Region and Its Urban Agglomerations. *Int. J. Appl. Earth Obs. Geoinf.* **2022**, *106*, 102643. [[CrossRef](#)]
51. Cao, J.J.; Cui, L. Current Status, Characteristics and Causes of Particulate Air Pollution in the Fenwei Plain, China: A Review. *J. Geophys. Res. Atmos.* **2021**, *126*, e2020JD034472. [[CrossRef](#)]
52. Liu, S.; Hua, S.; Wang, K.; Qiu, P.; Liu, H.; Wu, B.; Shao, P.; Liu, X.; Wu, Y.; Xue, Y.; et al. Spatial-Temporal Variation Characteristics of Air Pollution in Henan of China: Localized Emission Inventory, WRF/Chem Simulations and Potential Source Contribution Analysis. *Sci. Total Environ.* **2018**, *624*, 396–406. [[CrossRef](#)] [[PubMed](#)]
53. Yu, F.; Wang, Q.; Yan, Q.; Jiang, N.; Wei, J.; Wei, Z.; Yin, S. Particle Size Distribution, Chemical Composition and Meteorological Factor Analysis: A Case Study during Wintertime Snow Cover in Zhengzhou, China. *Atmos. Res.* **2018**, *202*, 140–147. [[CrossRef](#)]
54. Zhou, X.; Li, Z.; Zhang, T.; Wang, F.; Tao, Y.; Zhang, X. Multisize Particulate Matter and Volatile Organic Compounds in Arid and Semiarid Areas of Northwest China. *Environ. Pollut.* **2022**, *300*, 118875. [[CrossRef](#)]
55. Jiang, W.; Gao, W.; Gao, X.; Ma, M.; Zhou, M.; Du, K.; Ma, X. Spatio-Temporal Heterogeneity of Air Pollution and Its Key Influencing Factors in the Yellow River Economic Belt of China from 2014 to 2019. *J. Environ. Manag.* **2021**, *296*, 113172. [[CrossRef](#)]
56. Mi, Y.; Sun, K.; Li, L.; Lei, Y.; Wu, S.; Tang, W.; Wang, Y.; Yang, J. Spatiotemporal Pattern Analysis of PM<sub>2.5</sub> and the Driving Factors in the Middle Yellow River Urban Agglomerations. *J. Clean. Prod.* **2021**, *299*, 126904. [[CrossRef](#)]
57. Guan, Q.; Cai, A.; Wang, F.; Yang, L.; Xu, C.; Liu, Z. Spatio-Temporal Variability of Particulate Matter in the Key Part of Gansu Province, Western China. *Environ. Pollut.* **2017**, *230*, 189–198. [[CrossRef](#)] [[PubMed](#)]
58. Wang, S.; Liao, T.; Wang, L.; Sun, Y. Process Analysis of Characteristics of the Boundary Layer during a Heavy Haze Pollution Episode in an Inland Megacity, China. *J. Environ. Sci.* **2016**, *40*, 138–144. [[CrossRef](#)]
59. He, Q.; Yan, Y.; Guo, L.; Zhang, Y.; Zhang, G.; Wang, X. Characterization and Source Analysis of Water-Soluble Inorganic Ionic Species in PM<sub>2.5</sub> in Taiyuan City, China. *Atmos. Res.* **2017**, *184*, 48–55. [[CrossRef](#)]
60. Zhang, Q.; Streets, D.G.; Carmichael, G.R.; He, K.B.; Huo, H.; Kannari, A.; Klimont, Z.; Park, I.S.; Reddy, S.; Fu, J.S.; et al. Asian Emissions in 2006 for the NASA INTEX-B Mission. *Atmos. Chem. Phys.* **2009**, *9*, 5131–5153. [[CrossRef](#)]
61. Wang, J.; Xu, C. GeoDetector: Principle and Prospective. *Acta Geogr. Sin.* **2017**, *72*, 116–134. [[CrossRef](#)]
62. Wang, J.F.; Hu, Y. Environmental Health Risk Detection with GeogDetector. *Environ. Model. Softw.* **2012**, *33*, 114–115. [[CrossRef](#)]
63. Cai, S.; Wang, Y.; Zhao, B.; Wang, S.; Chang, X.; Hao, J. The Impact of the “Air Pollution Prevention and Control Action Plan” on PM<sub>2.5</sub> Concentrations in Jing-Jin-Ji Region during 2012–2020. *Sci. Total Environ.* **2017**, *580*, 197–209. [[CrossRef](#)] [[PubMed](#)]
64. Jiang, X.; Hong, C.; Zheng, Y.; Zheng, B.; Guan, D.; Gouldson, A.; Zhang, Q.; He, K. To What Extent Can China’s near-Term Air Pollution Control Policy Protect Air Quality and Human Health? A Case Study of the Pearl River Delta Region. *Environ. Res. Lett.* **2015**, *10*, 104006. [[CrossRef](#)]
65. Zhan, D.; Kwan, M.P.; Zhang, W.; Yu, X.; Meng, B.; Liu, Q. The Driving Factors of Air Quality Index in China. *J. Clean. Prod.* **2018**, *197*, 1342–1351. [[CrossRef](#)]
66. Teng, T.; Chen, D.; Hu, S. Spatial Evolution and Influencing Factors of Spatial Agglomeration Pattern of Air Pollution in the Yellow River Basin. *Sci. Geogr. Sin.* **2021**, *41*, 1852–1861. [[CrossRef](#)]
67. Li, H.; Han, Y. Analysis on the Spatial-Temporal Evolution Characteristics of PM<sub>2.5</sub> and Its Influencing Factors in the Yellow River Basin. *World Reg. Stud.* **2022**, *31*, 130–141.
68. Hsu, C.H.; Cheng, F.Y. Classification of Weather Patterns to Study the Influence of Meteorological Characteristics on PM<sub>2.5</sub> Concentrations in Yunlin County, Taiwan. *Atmos. Environ.* **2016**, *144*, 397–408. [[CrossRef](#)]
69. Duo, B.; Zhang, Y.; Kong, L.; Fu, H.; Hu, Y.; Chen, J.; Li, L.; Qiong, A. Individual Particle Analysis of Aerosols Collected at Lhasa City in the Tibetan Plateau. *J. Environ. Sci.* **2015**, *29*, 165–177. [[CrossRef](#)]
70. Duo, B.; Cui, L.; Wang, Z.; Li, R.; Zhang, L.; Fu, H.; Chen, J.; Zhang, H.; Qiong, A. Observations of Atmospheric Pollutants at Lhasa during 2014–2015: Pollution Status and the Influence of Meteorological Factors. *J. Environ. Sci.* **2018**, *63*, 28–42. [[CrossRef](#)]
71. Chen, Z.; Chen, D.; Zhao, C.; Kwan, M.-P.; Cai, J.; Zhuang, Y.; Zhao, B.; Wang, X.; Chen, B.; Yang, J.; et al. Influence of Meteorological Conditions on PM<sub>2.5</sub> Concentrations across China: A Review of Methodology and Mechanism. *Environ. Int.* **2020**, *139*, 105558. [[CrossRef](#)] [[PubMed](#)]
72. Yang, X.; Zhao, C.; Zhou, L.; Wang, Y.; Liu, X. Distinct Impact of Different Types of Aerosols on Surface Solar Radiation in China. *J. Geophys. Res. Atmos.* **2016**, *121*, 6459–6471. [[CrossRef](#)]
73. Zhang, W.; Wang, H.; Zhang, X.; Peng, Y.; Zhong, J.; Wang, Y.; Zhao, Y. Evaluating the Contributions of Changed Meteorological Conditions and Emission to Substantial Reductions of PM<sub>2.5</sub> Concentration from Winter 2016 to 2017 in Central and Eastern China. *Sci. Total Environ.* **2020**, *716*, 136892. [[CrossRef](#)]

74. Zhang, Q.; Quan, J.; Tie, X.; Li, X.; Liu, Q.; Gao, Y.; Zhao, D. Effects of Meteorology and Secondary Particle Formation on Visibility during Heavy Haze Events in Beijing, China. *Sci. Total Environ.* **2015**, *502*, 578–584. [[CrossRef](#)]
75. Zhong, J.; Zhang, X.; Wang, Y.; Sun, J.; Zhang, Y.; Wang, J.; Tan, K.; Shen, X.; Che, H.; Zhang, L.; et al. Relative Contributions of Boundary-Layer Meteorological Factors to the Explosive Growth of PM<sub>2.5</sub> during the Red-Alert Heavy Pollution Episodes in Beijing in December 2016. *J. Meteorol. Res.* **2017**, *31*, 809–819. [[CrossRef](#)]
76. Peng, Z.-R.; Wang, D.; Wang, Z.; Gao, Y.; Lu, S. A Study of Vertical Distribution Patterns of PM<sub>2.5</sub> Concentrations Based on Ambient Monitoring with Unmanned Aerial Vehicles: A Case in Hangzhou, China. *Atmos. Environ.* **2015**, *123*, 357–369. [[CrossRef](#)]
77. Zhang, C.; Ni, Z.; Ni, L. Multifractal Detrended Cross-Correlation Analysis between PM<sub>2.5</sub> and Meteorological Factors. *Phys. A Stat. Mech. Its Appl.* **2015**, *438*, 114–123. [[CrossRef](#)]
78. Fang, C.; Zhang, Z.; Jin, M.; Zou, P.; Wang, J. Pollution Characteristics of PM<sub>2.5</sub> Aerosol during Haze Periods in Changchun, China. *Aerosol Air Qual. Res.* **2017**, *17*, 888–895. [[CrossRef](#)]
79. Song, S.; Gao, M.; Xu, W.; Sun, Y.; Worsnop, D.R.; Jayne, J.T.; Zhang, Y.; Zhu, L.; Li, M.; Zhou, Z.; et al. Possible Heterogeneous Chemistry of Hydroxymethanesulfonate (HMS) in Northern China Winter Haze. *Atmos. Chem. Phys.* **2019**, *19*, 1357–1371. [[CrossRef](#)]
80. Tie, X.; Huang, R.-J.; Cao, J.; Zhang, Q.; Cheng, Y.; Su, H.; Chang, D.; Pöschl, U.; Hoffmann, T.; Dusek, U.; et al. Severe Pollution in China Amplified by Atmospheric Moisture. *Sci. Rep.* **2017**, *7*, 15760. [[CrossRef](#)]
81. Zhai, S.; Jacob, D.J.; Wang, X.; Shen, L.; Li, K.; Zhang, Y.; Gui, K.; Zhao, T.; Liao, H. Fine Particulate Matter (PM<sub>2.5</sub>) Trends in China, 2013–2018. Separating Contributions from Anthropogenic Emissions and Meteorology. *Atmos. Chem. Phys.* **2019**, *19*, 11031–11041. [[CrossRef](#)]
82. Zheng, B.; Zhang, Q.; Zhang, Y.; He, K.B.; Wang, K.; Zheng, G.J.; Duan, F.K.; Ma, Y.L.; Kimoto, T. Heterogeneous Chemistry: A Mechanism Missing in Current Models to Explain Secondary Inorganic Aerosol Formation during the January 2013 Haze Episode in North China. *Atmos. Chem. Phys.* **2015**, *15*, 2031–2049. [[CrossRef](#)]
83. Gao, M.; Liu, Z.; Wang, Y.; Lu, X.; Ji, D.; Wang, L.; Li, M.; Wang, Z.; Zhang, Q.; Carmichael, G.R. Distinguishing the Roles of Meteorology, Emission Control Measures, Regional Transport, and Co-Benefits of Reduced Aerosol Feedbacks in “APEC Blue”. *Atmos. Environ.* **2017**, *167*, 476–486. [[CrossRef](#)]
84. Li, W.; Liu, X.; Zhang, Y.; Sun, K.; Wu, Y.; Xue, R.; Zeng, L.; Qu, Y.; An, J. Characteristics and Formation Mechanism of Regional Haze Episodes in the Pearl River Delta of China. *J. Environ. Sci.* **2018**, *63*, 236–249. [[CrossRef](#)] [[PubMed](#)]
85. Song, H.; Zhang, K.; Piao, S.; Liu, L.; Wang, Y.P.; Chen, Y.; Yang, Z.; Zhu, L.; Wan, S. Soil Organic Carbon and Nutrient Losses Resulted from Spring Dust Emissions in Northern China. *Atmos. Environ.* **2019**, *213*, 585–596. [[CrossRef](#)]
86. Yan, W.; Yang, L.; Chen, J.; Wang, X.; Wen, L.; Zhao, T.; Wang, W. Aerosol Optical Properties at Urban and Coastal Sites in Shandong Province, Northern China. *Atmos. Res.* **2017**, *188*, 39–47. [[CrossRef](#)]
87. Liu, L.; Zhang, X.; Zhong, J.; Wang, J.; Yang, Y. The ‘Two-Way Feedback Mechanism’ between Unfavorable Meteorological Conditions and Cumulative PM<sub>2.5</sub> Mass Existing in Polluted Areas South of Beijing. *Atmos. Environ.* **2019**, *208*, 1–9. [[CrossRef](#)]
88. Ren, Y.; Zheng, S.; Wei, W.; Wu, B.; Zhang, H.; Cai, X.; Song, Y. Characteristics of Turbulent Transfer during Episodes of Heavy Haze Pollution in Beijing in Winter 2016/17. *J. Meteorol. Res.* **2018**, *32*, 69–80. [[CrossRef](#)]
89. Yang, T.; Gbaguidi, A.; Yan, P.; Zhang, W.; Zhu, L.; Yao, X.; Wang, Z.; Chen, H. Model Elucidating the Sources and Formation Mechanisms of Severe Haze Pollution over Northeast Mega-City Cluster in China. *Environ. Pollut.* **2017**, *230*, 692–700. [[CrossRef](#)]
90. Zhong, J.; Zhang, X.; Dong, Y.; Wang, Y.; Liu, C.; Wang, J.; Zhang, Y.; Che, H. Feedback Effects of Boundary-Layer Meteorological Factors on Cumulative Explosive Growth of PM<sub>2.5</sub> during Winter Heavy Pollution Episodes in Beijing from 2013 to 2016. *Atmos. Chem. Phys.* **2018**, *18*, 247–258. [[CrossRef](#)]
91. Wu, Y.; Gu, B.; Erisman, J.W.; Reis, S.; Fang, Y.; Lu, X.; Zhang, X. PM<sub>2.5</sub> Pollution Is Substantially Affected by Ammonia Emissions in China. *Environ. Pollut.* **2016**, *218*, 86–94. [[CrossRef](#)] [[PubMed](#)]
92. Aksoyoglu, S.; Keller, J.; Barmpadimos, I.; Oderbolz, D.; Lanz, V.A.; Prévôt, A.S.H.; Baltensperger, U. Aerosol Modelling in Europe with a Focus on Switzerland during Summer and Winter Episodes. *Atmos. Chem. Phys.* **2011**, *11*, 7355–7373. [[CrossRef](#)]
93. Bray, C.D.; Battye, W.; Aneja, V.P.; Tong, D.Q.; Lee, P.; Tang, Y. Ammonia Emissions from Biomass Burning in the Continental United States. *Atmos. Environ.* **2018**, *187*, 50–61. [[CrossRef](#)]
94. Wang, C.; Yin, S.; Bai, L.; Zhang, X.; Gu, X.; Zhang, H.; Lu, Q.; Zhang, R. High-Resolution Ammonia Emission Inventories with Comprehensive Analysis and Evaluation in Henan, China, 2006–2016. *Atmos. Environ.* **2018**, *193*, 11–23. [[CrossRef](#)]
95. Li, M.; Liu, H.; Geng, G.; Hong, C.; Liu, F.; Song, Y.; Tong, D.; Zheng, B.; Cui, H.; Man, H.; et al. Anthropogenic Emission Inventories in China: A Review. *Natl. Sci. Rev.* **2017**, *4*, 834–866. [[CrossRef](#)]
96. Ti, C.; Han, X.; Chang, S.X.; Peng, L.; Xia, L.; Yan, X. Mitigation of Agricultural NH<sub>3</sub> Emissions Reduces PM<sub>2.5</sub> Pollution in China: A Finer Scale Analysis. *J. Clean. Prod.* **2022**, *350*, 131507. [[CrossRef](#)]
97. Vayenas, D.V.; Takahama, S.; Davidson, C.I.; Pandis, S.N. Simulation of the Thermodynamics and Removal Processes in the Sulfate-Ammonia-Nitric Acid System during Winter: Implications for PM<sub>2.5</sub> Control Strategies. *J. Geophys. Res. Atmos.* **2005**, *110*, D07S14. [[CrossRef](#)]
98. Zhou, Y.; Cheng, S.; Lang, J.; Chen, D.; Zhao, B.; Liu, C.; Xu, R.; Li, T. A Comprehensive Ammonia Emission Inventory with High-Resolution and Its Evaluation in the Beijing-Tianjin-Hebei (BTH) Region, China. *Atmos. Environ.* **2015**, *106*, 305–317. [[CrossRef](#)]

99. Wu, J.; Xie, W.; Li, W.; Li, J. Effects of Urban Landscape Pattern on PM<sub>2.5</sub> Pollution-A Beijing Case Study. *PLoS ONE* **2015**, *10*, e0142449. [[CrossRef](#)]
100. Yu, L.; Wang, G.; Zhang, R.; Zhang, L.; Song, Y.; Wu, B.; Li, X.; An, K.; Chu, J. Characterization and Source Apportionment of PM<sub>2.5</sub> in an Urban Environment in Beijing. *Aerosol Air Qual. Res.* **2013**, *13*, 574–583. [[CrossRef](#)]
101. Zhou, S.; Lin, R. Spatial-Temporal Heterogeneity of Air Pollution: The Relationship between Built Environment and on-Road PM<sub>2.5</sub> at Micro Scale. *Transp. Res. Part D Transp. Environ.* **2019**, *76*, 305–322. [[CrossRef](#)]